

Universal method to extract the average electron spin relaxation in organic semiconductors from muonium ALC resonances

Licheng Zhang,¹ J. S. Lord,^{2,*} and A. J. Drew^{1,†}

¹*School of Physical and Chemical Sciences, Queen Mary University of London, London, E1 4NS, UK*

²*ISIS Muon and Neutron Source, STFC, Rutherford Appleton Laboratory, Harwell Campus, Didcot, OX11 0QX, UK*

Muon spin spectroscopy and in particular the avoided level crossing (ALC) technique is a sensitive probe of electron spin relaxation (eSR) in organic semiconductors. In complex ALC spectra, eSR can be challenging to extract, as it requires the modelling of overlapping ALCs, where covariance between parameters can result in significant uncertainties. Here we demonstrate a general method to extract eSR rate, which is independent on the number of ALCs resonances present, whether they overlap or not, and what the muonium hyperfine (isotropic and anisotropic) parameters are. This can then be used to extract an accurate value for eSR rate and as guidance for undertaking experiments efficiently.

Spin interactions are vital to many applications of organic semiconductors (OSC), such as organic spintronics [1, 2], display technologies [3] and photovoltaics [4], with important mechanisms such as the various unpaired electron spin relaxation mechanisms, inter-system crossing, singlet fission and thermally activated delayed fluorescence (TADF) [5]. Having an accurate measurement of the electron spin relaxation time, τ_e , that can be applied to a wide variety of molecules is vital for developing these technologies, but also an interest in its own right. Experimental measurements of τ_e in OSC vary between a less than a microsecond to potentially second or more [6–8].

Electron paramagnetic resonance (EPR) is capable of providing a measure of τ_e , but it requires a material with intrinsic unpaired electrons or electrons provided by doping, which is not always possible. τ_e can also be extracted from magnetotransport measurements on unipolar spin valve devices [9, 10], but this approach requires a robust theoretical model. For example, models that build on the Elliott-Yafet [11] or Dyakonov-Perel mechanisms [12], or one involving electrons observing a random hyperfine field upon hopping between molecular sites [13]. There are a number of issues with many of the earlier theoretical models. They are usually most applicable to band semiconductors, which are likely not suited to the localised molecular orbitals in OSC. All of the theoretical models that are transport based that require an accurate measure of the charge carrier mobility, whose uncertainty even in well-defined organic light emitting diodes (OLED) leads to a significant uncertainties in the value of τ_e . The strong temperature dependence of charge carrier mobility also often obscures the underlying physics of the spin relaxation mechanisms.

Harmon et al. have produced a theory for spin relaxation of hopping carriers in a disordered organic semiconductor, that considers hopping induced eSR from spin-orbit coupling (SOC) and the hyperfine interaction (HFI) and an “intrasite”, or intramolecular, spin relaxation

mechanism involving spin-lattice interactions (time varying HFI) but not SOC [14]. Charge carrier mobility in OSC, especially in devices where the OSC is amorphous, is low; the charge carrier resides on the molecule for a significant amount of time, and it is not clear whether the hopping or intramolecular mechanisms are dominant under what limits in real-world OSC. Experimental verification is needed. More recently, a particularly elegant systematic but primarily theoretical study has been carried out that demonstrates a rich variability of the g-shifts with the effective SOC [8], which is dependant on subtle aspects of molecular composition and structure. The work was carried out in isolated molecules and the authors note their results are likely to be relevant in solid state systems, although this is not 100% clear and would also benefit from being experimentally determined. In general, for intramolecular interactions, the relative importance of SOC or HFI has not been properly addressed experimentally.

Muon spin resonance (μ SR), also known as avoided level crossing (ALC) spectroscopy, has been demonstrated to be an excellent probe of spin dynamics in OSC [15–19] in the solid state and liquid/solution state, but to extract eSR requires modelling and for complex signals, this is not always possible[20]. Importantly, it measures the intramolecular eSR, and not one based on hopping, and so is an ideal technique to study the intrinsic interactions responsible for eSR. In a muon experiment, a 100% spin polarised positively charged muon beam is implanted into the sample. In OSC (and certain other materials), the muon can capture an electron to form a muonium atom. It loses some of its polarisation as a result of HFI between the muon and electron that result in Rabi oscillations. Muonium is often referred to as light hydrogen, by virtue of its ionisation energy and chemical reactions being similar to hydrogen, but is around 9 times lighter [21]. In most OSC, muonium chemically bonds to a molecule (often referred to as a “muoniated radical” [22]), where the muon-electron HFI is smaller, due to the spreading out of the electron’s wavefunction on the molecule. It is worth noting that in this case, the technique self dopes an electron to the molecule, and so

* James.Lord@stfc.ac.uk

† A.J.Drew@qmul.ac.uk

is applicable to the majority of OSC, unlike EPR. A relaxation of this electron’s spin can induce changes in the muon spin, which are then subsequently detected [18]. The muon and muonium have a half-life of $2.2 \mu\text{s}$, decaying into a positron that is correlated to the muon’s spin at the time of decay. By measuring the time dependence of the spatial distribution of emitted positrons, one is able to extract a direct measurement of the spin polarization of the ensemble of muons, and thus a measure of the electron spin dynamics in the sample.

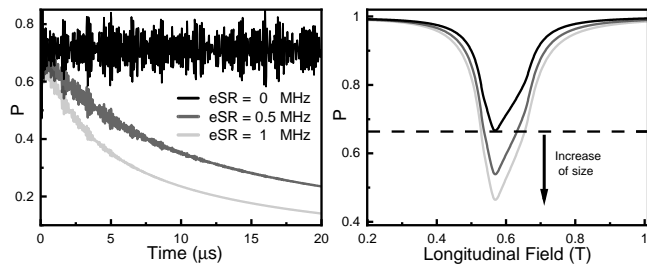


FIG. 1. The influence of the dynamical effect of the electron near an ALC (HFCC $A = 160\text{MHz}$, $D = 20\text{MHz}$, $E = 10\text{MHz}$). (a) The eSR effects a reduction of the muon spin polarization over time. $B = 0.6\text{T}$. (b) Time integral of the muon spin polarization curves.

In a typical solid-state experiment in a polycrystalline OSC, one applies a magnetic field parallel with the muon’s initial spin direction, termed a longitudinal field (LF). The energy levels of the singlet/triplet bound muonium states are tuned via the Zeeman interaction. This has two main effects. Firstly it slowly decouples the muon’s spin from the electron’s spin as the externally applied field scales with the internal muon-electron HFI (randomly oriented with respect to the LF), known as repolarisation. Secondly, in high magnetic fields, where most attempts to measure τ_e are carried out, the eigenstates of the spin systems are to a good approximation pure Zeeman product states. Muons injected with their spins parallel or anti-parallel to the field are thus in an eigenstate, and no time evolution of spin polarization is expected. At a particular longitudinal field cross relaxation effects produce an avoided level crossing (ALC), at what would otherwise be energy level degeneracies; the $m_s=1$ and $m_s=0$ triplet eigenstates are mixtures between two Zeeman states. This leads to an oscillation between the levels. Whenever the two mixing levels belong to different muon magnetic quantum states, the time evolution causes a depolarization of the muon’s spin. The muon technique is particularly sensitive to eSR whilst on an ALC resonance, as this loss of spin polarisation is “locked in” as the $m_s=-1$ triplet state is off-resonance [18, 22].

In the solid state, the positions and linewidths of the ALC resonances are determined by the muon-electron isotropic and anisotropic HFI, which means that different muonium bonding sites on the molecules will have different ALC resonances. Further details can be found

elsewhere [18, 22, 23]. It has been demonstrated that eSR probed with the muonium electron via ALC spectroscopy are governed by the same mechanisms in OLEDs and optical spectroscopy [17], opening up a world of opportunity to study OSC and suggesting that these effects are dominated by intramolecular mechanisms.

eSR is strongly temperature dependent because it is driven by vibrations. Typically when performing an experiment, one would measure an ALC spectra at a low temperature (e.g 10K), followed by the higher temperatures at which eSR is to be measured. One then assumes a negligibly small eSR at low temperatures to extract the eSR at high temperatures. This assumes that temperature dependent changes to muonium formation are negligible, which can be checked by transverse field measurements and by studying more than one ALC resonance (if available, and sufficiently separated in magnetic field). It is thus a good technique to extract detailed information on how SOC depends on subtle aspects of molecular composition and structure in the solid state [8]. However, one of the main problems with using ALC μSR to probe eSR in the solid state is that often, there are overlapping ALC resonances from different muonium bonding sites, that can make fitting or modelling challenging [17]. It can be difficult to extract the full anisotropic technique hyperfine parameters of the different states needed to extract the eSR and there is covariance between parameters. In the extreme limit, this limitation can obscure the results entirely [24]. Even in better behaved systems, there is evidence that there is a distribution of bonding angles meaning a distribution of muon-electron HFI [25, 26]. In any experiment, it can be extremely hard to justify enough time on a muon instrument to measure the complete temperature dependence with sufficient number of data points on the ALCs to extract the temperature dependent eSR. Previously, a single-point tracking of the ALC amplitude as a function of temperature has been used [15], but if the data involves overlapping peaks or the peak position is a function of temperature (muon-electron HFI may be a function of temperature), then this method is challenging and likely won’t yield satisfactory results.

Here, we demonstrate these limitations explicitly and demonstrate a new method to deal with some of the challenging data sets discussed above. We demonstrate that by proper handling of the data, one is able to use a universal law to extract the eSR, that is independent of the technique hyperfine parameters (and thus their temperature or bonding angle dependence) and the complexity or overlap of the ALC resonance spectra (and thus is applicable for even the extreme cases [24]). We then test it against a known and published data-set originally analysed using the historical modelling methodology.

We used the Quantum software [27, 28] to model LF dependence of the muon’s polarisation, $P(t)$, as a function of eSR, the isotropic (A) and anisotropic (D , E) hyperfine coupling constants (see [18] for a longer discussion) and for different combinations of ALCs with differ-

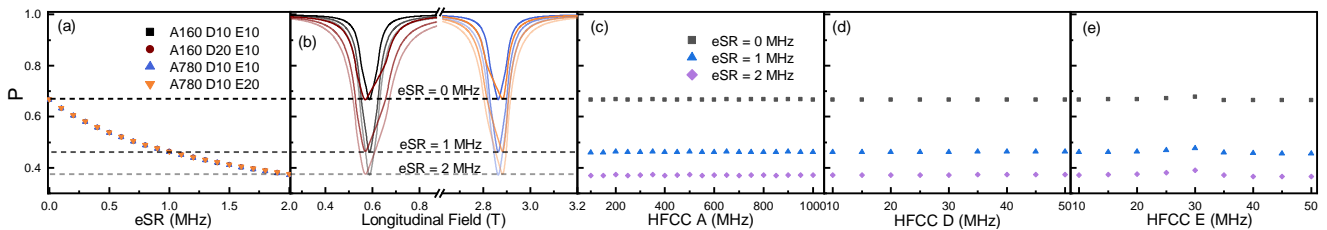


FIG. 2. (a) The time-integral minimum polarisation versus eSR. (b) The corresponding time integral of the muon spin polarization curves with different eSR in 4 models. (c-e) The time-integral minimum polarisation versus HFCC A, D and E. (c) $D = 10\text{MHz}$ and $E = 10\text{MHz}$. (d) $A = 780\text{MHz}$ and $E = 10\text{MHz}$. (e) $A = 780\text{MHz}$ and $D = 10\text{MHz}$. P is polarisation and P_{min} is the minimum polarisation (center of the ALC).

ent muon-electron hyperfine constants. Quantum models the muon together with nearby spins such as electrons and nuclei, interacting via dipolar, hyperfine and quadrupolar interactions, taking into account of Zeeman interaction with both static and RF magnetic fields, and spin flips and site changes. It uses an effective Hamiltonian where the dynamic changes (e.g spin flips or site changes) are handled by a density matrix approach with exponential relaxation rates. Then different muonium sites are calculated independently, and combined to form a final field dependent signal to compare to the experimental data.

Shown in Figure 1(a) is an example of the time dependence of the muon’s polarisation, where it can be seen that the (fast) Rabi oscillations are present at all values of eSR, superimposed on the relaxation rate brought about by eSR. In most experiments, the Rabi oscillations are averaged out and not observed. A common way to plot the ALC resonance data taken on time differential (TD) muon spectrometers is to integrate the time dependent spectra. This is without detrimental effect to the underlying physics of the sample in most cases, but one must be aware of a few different effects. Firstly, the modelling and data analysis become easier, by virtue of only needing to worry about the model independent time integral (TI) ALC. The overall statistics needed to be taken is lower because fitting in the time domain is model dependent and tends to weight slightly more at higher times, resulting in larger errors on parameters (in particular, the asymmetry). At pulsed muon sources, TI detector deadtime is less apparent than TD, allowing a greater acquisition rate. This makes beamtime more efficient, although large deadtime can still introduce non-linearities between the actual TI asymmetry and the measured one.

Modelled TI asymmetry for some typical values of eSR is shown in Figure 1(b). The amplitude of the ALCs increases as eSR increases, due to the exponential polarisation loss related to the coupling of the muon’s and electron’s spins. An experimentally convenient proxy therefore for measuring eSR is the amplitude of the ALC resonance (i.e minimum polarisation, P_{min}) [15]. For those materials where the ALC position is not particularly temperature dependent, eSR can be extracted as a function of temperature by a single point measurement of P_{min} ,

with only full-field scans of the ALCs taken at a limited number of temperatures, saving a significant amount of experimental time [15]. This technique has been demonstrated in our modelling; P_{min} is shown as a function of eSR for various A, D and E’s in Figure 2(a), with the corresponding ALC resonances in Figures 2(a) and (b). It is clear from the overlapping points in Figure 2(a), that the eSR extracted from P_{min} is independent of A, D or E. Figure 2 (d)-(f) demonstrates that P_{min} shows minimal dependence on A, D or E over the parameter space relevant to the majority of muoniated radicals in OSCs. We can therefore extract eSR from single point measurements, once properly normalised (to the eSR = 0 assumption at low temperature [15]), if the ALC resonance doesn’t move with temperature and there is only one dominant ALC resonance at the field chosen. It is worth noting that for the majority of experiments on solid state OSC, these conditions are not met.

Muon-electron hyperfine coupling constants can vary considerably between different muon adducts, even ones that are next to each other on the same molecule. For many molecular systems, several ALC resonances can overlap and form a wider and more complex signal; it is particularly a problem for those systems with large D and/or E, yielding merged and ill-defined ALC data. We have calculated these effects for 1 or 2 ALC resonances using reasonable estimates of parameters, shown in Fig. 3(a)-(d) - a single ALC resonance used for benchmarking, and MIX1, MIX2 and MIX3 containing different combinations of ALC resonances. MIX1 is the combination of two ALC resonances of equal weight that are separated by a significant margin, but, still have their ‘tails’ overlapping with each other in the field range between the two. MIX2 and MIX3 are the combination of two much closer ALC resonances, with the difference between MIX2 and MIX3 being the ratio of the two amplitudes.

In Fig. 3(e), we can see the P_{min} now has dependence on the specifics of the ALCs being measured, making extraction of eSR from it challenging. The majority of the difference between the benchmark and MIX1-3, is related to the signal being split between several ALCs. In typical experimental analysis, this would be normalised out. We define the maximum polarization loss ratio, R_{PL} , as $R_{PL} = \frac{PL_{eSR}}{PL_0}$, where $PL_{eSR} = 1 - P_{min}$ with a non-zero

eSR and $PL_0 = 1 - P_{min}$ with zero eSR. This is similar to the normalisation techniques used on real experimental data, and the outcome is shown in Figure 3(f). It can be seen that MIX1 (separated ALCs) now sits nicely onto the benchmark, but the other two do not. This unambiguously demonstrates that it is possible to improve efficiency of the temperature dependent measurements of the estimate the eSR by taking a single point on the ALC as a function of temperature, when the temperature dependence of A is small, there is only one ALC line dominating the signal and when eSR is relatively small.

There another step we can take to improve matters. We define an integrated polarization loss ratio (meaning the ratio of integrated ALC resonances for finite eSR and 0 eSR) as

$$R_{IPL} = \frac{\sum_{B_{min}}^{B_{max}} PL_{eSR}(B_i) \Delta B_i}{\sum_{B_{min}}^{B_{max}} PL_0(B_j) \Delta B_j} \quad (1)$$

where B_{min} and B_{max} the minimum and maximum fields, chosen to minimise the systematic errors (see the Supplementary Material for how to choose them), $PL_{eSR}(B_i)$ and $PL_0(B_j)$ are the polarisation loss for the model with eSR at the longitudinal fields, B_i , and without eSR at the longitudinal fields, B_j . $\Delta B_i = \frac{1}{2}(B_{i+1} - B_{i-1})$. R_{IPL} is shown in Fig. 3(g), where it is clear that the change in area underneath the ALC is independent of the technique hyperfine couplings (A,D,E), the number of ALCs present and whether they overlap or not. This therefore represents generalised tool, where the eSR falls onto a single universal law. It has the potential to simplify the analysis significantly.

To understand the physics of how R_{IPL} varies with eSR, we consider the following model. Without any eSR, only the radicals with electron spin up can contribute to the muon's relaxation. With sufficient relaxation that the electron is almost certain to be flipped in the muon lifetime (so initially spin down ones then contribute to the integral asymmetry), but still slow enough compared to the muon-electron hyperfine constants that it doesn't effect the linewidth much, but does effect the overall amplitude. We would expect this to have a functional form of $R_A = 2 - \exp(-\tau_\mu eSR/2)$. The difference between R_{IPL} and R_A is shown in Figure Fig. 3(h), where there is good agreement below about $1/\tau_\mu$, indicating that the primary effect at low eSR is amplitude. Now turning to the width increase as eSR gets larger, above $1/\tau_\mu$, when off the line centre the muon's polarisation oscillates around a value between 1/2 and 1. Flipping the electron to spin down results in the polarisation being "frozen" (strictly the longitudinal part is frozen parallel to B and the perpendicular parts are dephased by rapid precession) and if you flip it again the muon oscillation starts again from a phase of "0 degrees", scaled down by the frozen value. So the line should broaden, since the central asymmetry is only doubled but the sides are enhanced more. We note that for any individual muon site (fixed angle with respect to the principal axes of

the muon-electron hyperfine tensor) the line is a simple Lorentzian $P = 1/2 + 1/2A^2/[(B - B_0)^2\gamma^2 + A^2]$, if $A > 1/\tau_\mu$, and it might give a simple answer dependent only on eSR, provided we also have $A > eSR$. To make further progress, a challenging integral is needed to be solved analytically, but in the supporting material we demonstrate the line-broadening appears to be roughly linear with eSR (within reasonable limits, below 5 MHz). For now, purely as an experimental tool, we report the best polynomial fit to this universal law as $eSR = \frac{1}{\tau_\mu} [1.982(R_{IPL} - 1) + 1.028(R_{IPL} - 1)^2]$, likely to be a Taylor expansion to an exponential function.

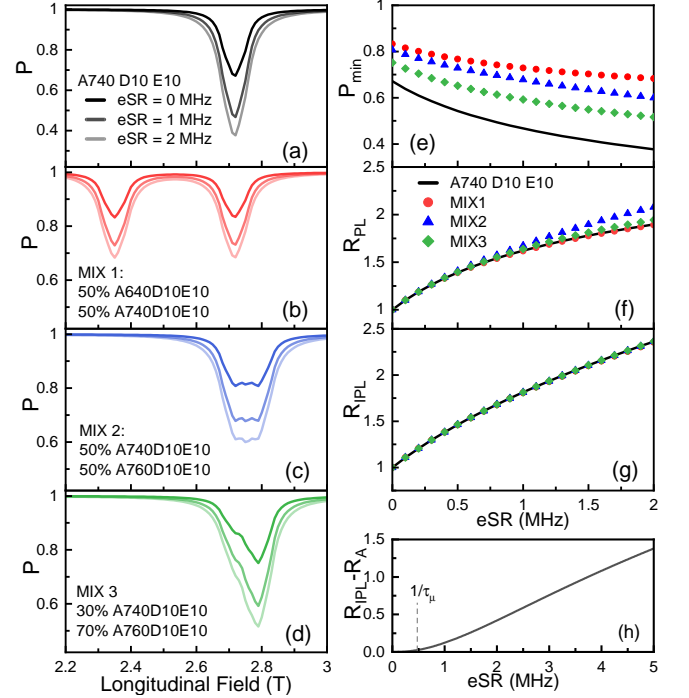


FIG. 3. (a)The single ALC resonance used for benchmark.(b)Two ALC resonances do not overlap. (c)(d)The same ALC resonances overlap with different composition.(e)-(g)The time-integral minimum polarisation, the minimum polarisation loss ratio and the integrated polarisation loss ratio versus eSR. (h) The difference between R_{IPL} and a simple amplitude-only model, showing a crossover to line broadening dominating R_{IPL} around $1/\tau_\mu$, which is roughly linear as eSR increases. See text.

In real experimental data, we usually cannot measure the full field range of the ALC resonances, since the 'tails' of the ALC resonance have a smaller amplitude than the experimental errors for a reasonable measurement time and the extended field ranges needed would add significantly to the required beam time. There is no one-size fits all for advising on the choice of the field range to measure (or analyse the data), as the widths of different ALC resonances are dependent on anisotropic HFCs, which are sample dependent. As a guide for experiments, how to deal with and define an effective field range (EFR) along with uncertainties introduced by having an too small an

EFR is discussed in the Supplementary Material.

To test our method on real data, we have analysed previously published work [15], which showed that eSR at room temperature (on the MHz scale) increased linearly with atomic number of the central atom of two metal-organic complexes, obtained via lineshape modelling of complex ALC spectra. One example ALC spectra is shown in Figure 4a. Figure 4b shows the difference between the eSR extracted using the previous modelling method and the method in this paper, for seven OSC containing metals of different atomic numbers. The eSR is plotted against the atomic number of the heaviest element on the molecule - the metal. There is strong agreement between the old and new methods.

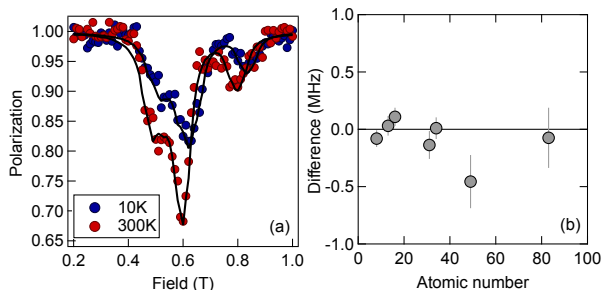


FIG. 4. (a) A relatively complex set of overlapping ALCs in triethylsilylethynyl anthradithiophene. Similar complexity and the same trends are present in all of the data in [17] (b) The difference between the new (this paper) and old ([17]) method of extracting eSR, plotted against the atomic number of the heaviest element in the molecule. There is clearly good agreement between the two methods. Seven samples in two series are shown: tris(8-hydroxyquinolato) Aluminium/Gallium/Indium/Bismuth and triethylsilylethynyl anthradifuran/anthradithiophene/anthradiselenophene. EFR was chosen to be the largest range available given the data, and varied from about 2.5 up to 10, depending on the dataset. The point at an atomic number of 50 appears to have a difference of 0.5MHz, although the uncertainties are large (mainly due to difficulty in modelling) and is still within 2σ .

There are a number of discussion points regarding this method. Whilst it is possible to handle a wider selection of data, in particular involving overlapping ALCs, it does only give you the average eSR of those overlapping ALCs (but if there are separated ALCs, then it's the average within each of those separated groups). Given for each

adduct the electron is potentially spatially restricted to different and specific parts of the molecule, this might result in different eSRs that are then averaged. This is particularly true for those molecules with heavy elements and a complex structure, as different adducts may result in different electron wavefunction overlap on the heavy element, different SOC, and thus different eSR. Modelling/fitting the ALC lineshapes and field dependent time series independently of one another may differentiate between the different eSR's and so should be the preference when undertaking analysis, but it is not always possible. Moreover, another source of relaxation such as impurities or structural changes modifying muonium sites or bonding probabilities/rates may significantly effect results.

There may also be issues with imperfect background subtraction; careful Ag backgrounds taken at all temperatures would help alleviate this problem, although these measurements are rarely perfect. If the background at different temperatures (or between samples) is identical in the raw data, then the effect will cancel out - this may be true for titanium cells for liquid experiments, but is unlikely the case for solid-state experiments in Ag packets. If an ALC falls on the repolarisation curve, most relevant in systems with at least two sites with one muon-electron isotropic HFI interaction being large and the other small, then the repolarisation curve can be treated as a background if it isn't possible to model it directly.

Nonetheless, this new analysis technique does have some significant advantages. In the case where complex ALC signals are present (overlapping ALCs) with similar eSRs then this gives us an additional tool in our analysis arsenal. In some cases we cannot ascertain whether a given ALC spectra is from an individual ALC resonance or several ALC resonances merged. Direct modelling in this case is challenging; single-point analysis of the temperature dependence may be impossible. This technique is particularly relevant in certain polymers, where significant structural disorder leads to unresolvable ALCs [24]. By comparing the results from R_{PL} with the R_{IPL} , we may be able to determine whether a particular experimental signal is a single ALC resonance or multiple overlapping ALC resonances, which is helpful to build a correct model. We would also be able to compare results from R_{IPL} with modelling to act as a benchmarking exercise; agreement between these two independent methods of extracting eSR would strengthen the conclusions that one can make from the modelling, and vice versa.

LZ acknowledges financial support from the Chinese Scholarship Council.

[1] W. Naber, S. Faez, and W. G. van der Wiel, Organic spintronics, *Journal of Physics D: Applied Physics* **40**, R205 (2007).
 [2] N. Morley, A. Rao, D. Dhandapani, M. Gibbs, M. Grell, and T. Richardson, Room temperature organic spintron-

ics, *Journal of Applied Physics* **103**, 07F306 (2008).
 [3] B. Geffroy, P. Le Roy, and C. Prat, Organic light-emitting diode (oled) technology: materials, devices and display technologies, *Polymer International* **55**, 572 (2006).
 [4] C. Brabec, U. Scherf, and V. Dyakonov, *Organic pho-*

tolvoltaics: materials, device physics, and manufacturing technologies (John Wiley & Sons, 2011).

- [5] S. R. Forrest, *Organic Electronics: Foundations to Applications* (Oxford University Press, 2021).
- [6] M. Cinchetti, K. Heimer, J.-P. Wüstenberg, O. Andreyev, M. Bauer, S. Lach, C. Ziegler, Y. Gao, and M. Aeschlimann, Determination of spin injection and transport in a ferromagnet/organic semiconductor heterojunction by two-photon photoemission, *Nature Materials* **8**, 115 (2009).
- [7] V. Dediu, M. Murgia, F. Maticotta, C. Taliani, and S. Barbanera, Room temperature spin polarized injection in organic semiconductor, *Solid State Communications* **122**, 181 (2002).
- [8] S. Schott, E. R. McNellis, C. B. Nielsen, *et al.*, Tuning the effective spin-orbit coupling in molecular semiconductors, *Nature Communications* **8**, 15200 (2017).
- [9] V. A. Dediu, L. E. Hueso, I. Bergenti, and C. Taliani, Spin routes in organic semiconductors, *Nature Materials* **8**, 707 (2009).
- [10] S. Pramanik, C.-G. Stefanita, S. Patibandla, S. Bandyopadhyay, *et al.*, Observation of extremely long spin relaxation times in an organic nanowire spin valve, *Nature Nanotechnology* **2**, 216 (2007).
- [11] R. Elliott, Theory of the effect of spin-orbit coupling on magnetic resonance in some semiconductors, *Physical Review* **96**, 266 (1954).
- [12] M. D'yakonov and V. Perel, Spin orientation of electrons associated with the interband absorption of light in semiconductors, *Soviet Journal of Experimental and Theoretical Physics* **33**, 1053 (1971).
- [13] P. Bobbert, W. Wagemans, F. Van Oost, B. Koopmans, *et al.*, Theory for spin diffusion in disordered organic semiconductors, *Physical Review Letters* **102**, 156604 (2009).
- [14] N. Harmon and M. Flatte, Distinguishing spin relaxation mechanisms in organic semiconductors, *Physical Review Letters* **110**, 176602 (2013).
- [15] L. Schulz, M. Willis, L. Nuccio, P. Shusharov, S. Fratini, F. Pratt, W. Gillin, T. Kreouzis, M. Heeney, N. Stingelin, *et al.*, Importance of intramolecular electron spin relaxation in small molecule semiconductors, *Physical Review B* **84**, 085209 (2011).
- [16] L. Nuccio, L. Schulz, M. Willis, F. L. Pratt, M. Heeney, N. Stingelin, C. Bernhard, and A. J. Drew, Electron spin relaxation in organic semiconductors probed through μ SR, *Journal of Physics: Conference Series* **292**, 012004 (2011).
- [17] L. Nuccio, M. Willis, L. Schulz, S. Fratini, F. Messina, M. D'Amico, F. L. Pratt, J. S. Lord, I. McKenzie, M. Loth, *et al.*, Importance of spin-orbit interaction for the electron spin relaxation in organic semiconductors, *Physical Review Letters* **110**, 216602 (2013).
- [18] L. Nuccio, L. Schulz, and A. Drew, Muon spin spectroscopy: magnetism, soft matter and the bridge between the two, *Journal of Physics D: Applied Physics* **47**, 473001 (2014).
- [19] S. Han, K. Wang, M. Willis, L. Nuccio, *et al.*, Muonium avoided level crossing measurement of electron spin relaxation rate in a series of substituted anthradithiophene based molecules, *Synthetic Metals* **208**, 39 (2015).
- [20] We note that we are exclusively considering Δ_1 resonances present in the solid state due to anisotropy, without the additional proton-electron coupling necessary for Δ_0 . Further details of different ALC states can be found in [18].
- [21] D. C. Walker and W. D. Walker, *Muon and muonium chemistry* (Cambridge University Press, 1983).
- [22] S. J. Blundell, Muon-spin rotation studies of electronic properties of molecular conductors and superconductors, *Chemical Reviews* **104**, 5717 (2004).
- [23] K. Wang, L. Schulz, M. Willis, S. Zhang, *et al.*, Spintronic and electronic phenomena in organic molecules measured with μ sr, *Journal of the Physical Society of Japan* **85**, 091011 (2016).
- [24] J. He, J. Du, T. Kreouzis, F. L. Pratt, *et al.*, Muon spin relaxation study of spin dynamics in poly (triarylamine), *Synthetic Metals* **208**, 21 (2015).
- [25] A. Adam Berlie, F. Pratt, B. Huddart, T. Lancaster, and S. Cottrell, Muon-nitrogen quadrupolar level crossing resonance in a charge transfer salt, *Journal of Physical Chemistry C* **126**, 7529 (2022).
- [26] L. Clowney, J. Jain, A. Srinivasan, J. Westbrook, W. Olson, and H. Berman, Geometric parameters in nucleic acids: Nitrogenous bases, *Journal of the American Chemical Society* **118**, 509 (1996).
- [27] J. Lord, Computer simulation of muon spin evolution, *Physica B: Condensed Matter* **374**, 472 (2006).
- [28] O. Arnold, J.-C. Bilheux, J. Borreguero, A. Buts, S. I. Campbell, L. Chapon, M. Doucet, N. Draper, R. F. Leal, M. Gigg, *et al.*, Mantid—data analysis and visualization package for neutron scattering and μ sr experiments, *Nuclear Instruments and Methods in Physics Research Section A: Accelerators, Spectrometers, Detectors and Associated Equipment* **764**, 156 (2014).